NATIONAL ADVISORY COMMITTEE
FOR AERONAUTICS

TECHNICAL NOTE 2107

INVESTIGATION OF FIRST STAGE OF TWO-STAGE TURBINE

DESIGNED FOR FREE-VORTEX FLOW

By G. W. Englert and A. O. Ross

Lewis Flight Propulsion Laboratory
Cleveland, Ohio

NACA

Washington
June 1950

NATIONAL ADVISORY COMMITTEE FOR AERONAUTICS

TECHNICAL NOTE 2107

INVESTIGATION OF FIRST STAGE OF TWO-STAGE TURBINE

DESIGNED FOR FREE-VORTEX FLOW

By G. W. Englert and A. O. Ross

SUMMARY

A preliminary experimental investigation was made of the first stage of a two-stage turbine designed for free-vortex flow. This stage was matched to a centrifugal compressor and was operated in conjunction with combustors, engine accessories, and three sizes of jet nozzle. Additional information concerning this stage was obtained by investigating the flow through a sector of the stator by means of a stationary-cascade apparatus. The data obtained were used to check the turbine design and to determine the characteristics of this stage for matching with the second stage of the turbine.

The results of this investigation showed that highest adiabatic efficiency was attained when the turbine was operating near the design total-pressure ratio. This experimentally attained maximum efficiency was approximately 5 percent lower, however, than the value of 0.90 assumed in the design calculations. The outlet flow angles at the mean radial sections of the stator and the rotor approximated the design values within 2.5°. Radial distributions of outlet angle corresponding to a free-vortex velocity distribution were not fully attained, however. Radial distributions of total pressure at the stator and rotor outlets were constant within experimental accuracy over the major portion of the radial distances, as designed. Boundary-layer build-up at the stator outlet was not so large as anticipated; the displacement thickness was only 0.16 inch at the hub or inner shroud and negligible at the tip or outer shroud compared with values of 0.30 and 0.12 inch, respectively, assumed in the design.

INTRODUCTION

Radial distributions of fluid velocity, pressure, and temperature into and out of the various rows of blades must be selected in the initial phases of the design of a turbine. The selection of combinations of these flow distributions along with suitable design

methods for obtaining the specified distributions can be guided by
the study of previous investigations. These investigations should
be ones in which the selection of combinations of these flow distri-
butions were incorporated in a turbine and experimentally checked to
determine the extent to which the turbine operated as desired.

An investigation was made at the Lewis laboratory of the first
stage of an NACA two-stage gas turbine designed for free-vortex flow
and constructed for use in a turbine-propeller experimental engine.
The results of this investigation, which are reported herein, were
used to determine the characteristics of the flow entering the sec-
ond stage of this turbine. Investigation of the first stage before
completion of the second stage not only permits less costly modi-
fication (if any) of the turbine, but in this case also permitted
more extensive instrumentation at the stage outlet because of less
space restriction. Additional information concerning this stage
was obtained by investigating the stator separately where more ade-
quate instrumentation could be provided because of less space restric-
tion at the stator outlet. Combining the results of these stator-flow
investigations with results obtained by studying the first stage of
the turbine as a unit permits the determination of flow character-
istics at the inlet to the rotor of this stage, and thus gives a
more complete description of the internal flow within this stage.

SYMBOLS

The following symbols are used in this report:

A   area, (sq ft)

c_p specific heat at constant pressure, (Btu/(lb)($^\circ$R))

F   thrust, (lb)

g   acceleration due to gravity, 32.17 (ft/sec^2)

p   absolute pressure, (lb/sq ft)

R   gas constant, 53.35 (lb-ft/(lb)($^\circ$R))

T   absolute temperature, ($^\circ$R)

u   blade velocity, (ft/sec)

V   absolute fluid velocity, (ft/sec)

W   gas velocity relative to rotating blade, (ft/sec)

w   weight-flow rate of fluid, (lb/sec)

α flow angle at which gas leaves stator blades; arc tan $\dfrac{V_{u,4}}{V_{x,4}}$, (deg)

$\quad$ (fig. 1)

β flow angle at which gas enters rotor blades relative to rotor,

$\quad$ arc tan $\dfrac{V_{u,4}-|u|_4}{V_{x,4}}$,(deg) (fig. 1)

γ ratio of specific heats

δ flow angle at which gas leaves rotor blades with respect to some

$\quad$ stationary part of turbine, arc tan $\dfrac{V_{u,5}}{V_{x,5}}$, (deg) (fig. 1)

η adiabatic efficiency

θ flow angle at which gas leaves rotor blades relative to rotor,

$\quad$ arc tan $\dfrac{V_{u,5}+|u|_5}{V_{x,5}}$, (deg) (fig. 1)

ρ density, (lb/cu ft)

Subscripts:

c   compressor

cr   critical, state at speed of sound (reference 1)

m   mean

n   normal to flow direction

T   turbine

u   tangential direction

x   axial direction

1,2,3, . . . 7   measuring stations (fig. 2)

Superscripts:

'   stagnation state

"   stagnation state relative to moving blades

BASIS OF DESIGN

The turbine investigated was designed for free-vortex flow distribution in which total pressure, total density, and vorticity (product of radius measured from the turbine axis times the tangential component of the absolute velocity of the gas at the particular radius) are constant in a radial direction from the hub to the tip of the turbine blades. It was assumed that the shift in mass rate of gas flow in a radial direction when passing through the turbine would be small, making the radial component of velocity of any one station negligible. This assumption combined with the condition of constant total pressure, total temperature, and vorticity produces a constant radial distribution of axial velocity from hub to tip (reference 2). The stator was designed for a uniform rectilinear-entrance-velocity distribution.

Inasmuch as the present investigation concerns only the first stage of this two-stage turbine, the first stage will hereinafter be considered as a complete single-stage turbine. The design inlet temperature, inlet pressure, and rotational speed were 1900° R, 8200 pounds per square foot, and 11,000 rpm, respectively. The design power output was 4130 horsepower and the assumed efficiency was 0.90. It was assumed that: (1) the losses across the stator would be negligible and all losses would occur across the rotor; (2) boundary layers having displacement thicknesses of 0.30 and 0.12 inch would be formed at the stator-outlet inner shroud and outer shroud, respectively; and (3) the inner boundary layer would be unstable in the rotor passages and reduced to zero at the rotor outlet (reference 2). A cross section of the turbine annulus in a plane passing through the axis of rotation showing the assumed boundary layers by shaded areas is shown in figure 3. The convergence and the divergence of the annular flow area are also shown on this figure. The minimum distance between the inner and outer shrouds is at the stator outlet. The outer shroud has a divergence angle of 9° from this station to the rotor exit and

a divergence angle of 6° from this same station to the stator entrance. The entrance to the stator was enlarged by this 6° divergence angle to accommodate the size of an existing burner-outlet assembly. The 9° divergence angle was used to limit the axial velocity components of the gas in passing through the turbine so that the vector sum of the velocity components at any particular station could be kept below a maximum critical-velocity ratio of 0.9, and yet permit the tangential velocities to attain values sufficient for the turbine to develop the desired power per pound of gas.

The blade profiles used in this turbine were designed by use of a stream-filament method given in reference 3. The coordinates according to which the blades were fabricated and the characteristic dimensions of the blades are shown in table I. The accuracy of fabrication was within ±0.010 inch; the inaccuracies were mainly due to the casting process. All blades had smooth profiles, however. There were 49 blades in the stator and 54 blades in the rotor.

APPARATUS AND PROCEDURE

Turbine Experiments

The turbine was matched to a centrifugal compressor, 14 combustors, and existing accessories in an arrangement similar to a turbojet engine, as shown in figure 2. The compressor originally had a double entry; however, the blades were machined from the back side and the flow passages faired in smoothly to reduce the weight flow and match the compressor with this turbine. Jet nozzles having diameters of 12.75, 13.78, and 15.97 inches were used successively as a means of varying turbine back pressure over the range expected to be obtained later during use of the second stage of the turbine. The engine was mounted on a test bed suspended by flexible cables, and thrust was measured by use of a strain gage. Total temperature was measured at the compressor inlet by means of six iron-constantan thermocouples, and at the compressor outlet by means of iron-constantan thermocouples located in two of 14 air adapters at the diffuser outlet. Total temperature was measured in the tail pipe by means of five shielded chromel-alumel thermocouples. Compressor-inlet pressure was the same as barometric pressure; compressor-outlet pressure was measured in two air adapters at the diffuser outlet by means of six total-pressure tubes. Turbine-inlet pressure was measured at three burner-outlet channels, two of which were in line with the two air adapters in which compressor-outlet pressure was measured. Total pressure at the turbine outlet and also the angle at

which the gas leaves the turbine were measured with a Feckheimer com-
bination total-pressure and yaw tube, shown in the enlarged section of
figure 2. This instrument was mounted in a remotely controlled actu-
ating device that enabled the operator to move the instrument in a
radial direction with respect to the turbine axis and also to rotate
the instrument about its own axis so that the yaw-tube readings could
be balanced (null method). The radial and angular positions of the
probe were determined by means of a self-balancing potentiometer.
The Feckheimer probe measurements were taken along one radial line
only. This radial line was approximately halfway between two
radial planes, that passing through the center of the top combustor
of the engine and that passing through the side of this same com-
bustor. Total pressure in the tail pipe was measured by three total-
pressure tubes and static pressure, by an orifice on the tail-pipe
wall. Static pressure at the turbine outlet was measured by wall
orifices on the inner and the outer turbine shrouds.

The rotational speeds at which the turbine was operated ranged
from 3980 to 11,400 rpm, and turbine-inlet temperature ranged from
1190° to 1950° R.

Stator-Cascade Experiments

The apparatus for investigating the stator flow (fig. 4) con-
sisted of a sector of an annular area in which five equally spaced
aluminum blades were mounted. The number of blades was limited to
five by the air capacity of the supply system. The ends of this
cascade of blades were wooden blocks with contours simulating an
adjacent blade profile so that there were six flow channels of equal
dimensions. The approach to the annular section consisted of a
wooden nozzle 11 inches long, mounted on a surge tank having a vol-
ume of 19 cubic feet. A pitot-static tube, located $2\frac{1}{2}$ inches upstream
of the blades, was so mounted that the entire area could be traversed
to check the inlet-flow distribution. A combination yaw, total-, and
static-pressure measuring probe (shown in enlarged section of fig. 4)
was positioned 0.1 inch downstream of the blades and mounted on a
protractor arrangement that permitted the probe to be so rotated that
the null method of balancing the yaw tubes could be used. This pro-
tractor was in turn mounted on a sliding mechanism adjustable by lead
screws so that the probe could be moved in two directions perpendi-
cular to one another in a plane normal to the axis of curvature of the
annular passage. Between the trailing edges of the center and the
next-to-center blades, 178 readings of static and total pressure and
flow direction were taken for each test condition. The pressure in
the surge tank was so regulated that the desired critical-velocity

ratio was obtained at the stator outlet. The temperature of the air in the surge tank was held at $580° \pm 2°$ R.

Data Computation

Turbine-inlet temperature. - Enthalpy drop in the turbine was found by equating it to the enthalpy increase in the compressor, which in turn was obtained from observations made with the instrumentation at stations 1 and 2 (fig. 2). It was assumed that the additional weight of fluid flowing through the turbine compared with that flowing through the compressor would balance the bearing friction and accessory power absorption. It was also assumed that the heat transfer through the tail pipe was negligible so that $T_5 = T_6 = T_7$. Turbine-inlet temperature can thus be found by the equation

$$T'_3 = T'_6 + \frac{c_{p,c}}{c_{p,T}} (T'_2 - T'_1) \tag{1}$$

where $c_{p,c}$ and $c_{p,T}$ are specific heats representative of the mean values in the compression process in the compressor and the expansion process in the turbine, respectively.

Turbine efficiency. - Turbine efficiency is reported as an adiabatic efficiency based on measured values of turbine-inlet and -outlet total pressure and measured outlet total temperature but calculated inlet temperature as follows:

$$\eta_T = \frac{T'_3 - T'_6 \text{ actual}}{T'_3 - T'_6 \text{ ideal}} = \frac{T'_3 - T'_6}{T'_3 \left[1 - \left(\frac{p'_5}{p'_3}\right)^{\frac{\gamma-1}{\gamma}} \right]} \tag{2}$$

where the mean specific heats through the ideal and actual processes are assumed equal.

Weight rate of fluid flow through turbine. - The weight rate of gas flow through the turbine was computed by means of the total- and

static-pressure, total-temperature, and area measurements taken in
the tail pipe (station 6). These values of weight flow were checked
against the weight flow computed by means of the thrust and static-
pressure measurements taken at the jet nozzle combined with the
total pressure and total temperature measured in the tail pipe. The
values of weight flow obtained by these two methods differed from
0.4 to 12.4 percent; the scatter in the data was generally at ran-
dom. The largest percentage of error was at the low values of
weight flow where the accuracy of the thrust gage reading probably
was not less than ±10 percent at the low values of thrust. The
first method of computation (based entirely on measurements taken
at station 6) was therefore considered more reliable and was used
in the engine weight-flow calculations for the data presented. The
equations used in these computations are derived as follows:

Weight flow based on station 6 measurements:

Continuity equation:

$$w = \rho VA$$

Isentropic relation:

$$\frac{\rho}{\rho'} = \left(\frac{p}{p'}\right)^{\frac{1}{\gamma}} = \left(\frac{T}{T'}\right)^{\frac{1}{\gamma-1}}$$

From the general energy equation,

$$T' = T + \frac{\gamma-1}{\gamma} \frac{V^2}{2gR}$$

Solving for V,

$$V = \sqrt{\frac{2\gamma gRT'}{(\gamma-1)} \left[1 - \left(\frac{p}{p'}\right)^{\frac{\gamma-1}{\gamma}}\right]} \tag{3}$$

Combination with the continuity and isentropic relation yields

$$w = A_6 p'_6{}^{\frac{\gamma-1}{\gamma}} \, p_6{}^{\frac{1}{\gamma}} \sqrt{\frac{2g}{(\gamma-1)RT'_6}\left[1 - \left(\frac{p_6}{p'_6}\right)^{\frac{\gamma-1}{\gamma}}\right]} \qquad (4)$$

Weight flow based on thrust measurements:

When the momentum equation

$$F = \frac{w}{g} V_7 \qquad (5)$$

is combined with equation (3) and solved for w,

$$w = \frac{gF}{\sqrt{\frac{2\gamma g RT'_6}{(\gamma-1)}\left[1 - \left(\frac{p_7}{p'_6}\right)^{\frac{\gamma-1}{\gamma}}\right]}} \qquad (6)$$

The use of this equation assumes that there is no change in total pressure or total temperature between stations 6 and 7.

Weight rate of fluid flow through stator cascade. - The weight rate of flow passing through the stator-cascade apparatus was computed by use of equation (4); total and static pressures were measured at the stator outlet and total temperature was measured in the surge tank. A corresponding increment of area was used for each pressure measurement and the total weight flow through the cascade was obtained by summation of the increments of weight flow.

Average critical-velocity ratio. - The average critical-velocity ratio at various stations in the turbine can be found from a knowledge of the weight flow through the turbine and the values of total pressure, total temperature, and flow direction at the station considered.

By use of the continuity equation and the isentropic relation between total and static densities and temperatures it is found that

$$\frac{W}{A_n V_{cr} \rho'} = \frac{\rho}{\rho'} = \left(\frac{T}{T'}\right)^{\frac{1}{\gamma-1}}$$

and because

$$T' = T + \frac{\gamma-1}{\gamma} \frac{V^2}{2gR}$$

and

$$V_{cr} = \sqrt{\frac{2\gamma}{\gamma+1} gRT'}$$

$$\frac{W}{A_n V_{cr} \rho'} = \frac{V}{V_{cr}} \left[1 - \frac{\gamma-1}{\gamma+1} \left(\frac{V}{V_{cr}}\right)^2\right]^{\frac{1}{\gamma-1}}$$

Inasmuch as these stagnation temperatures and pressures were measured with reference to some stationary part of the turbine only, additional relations are needed to obtain the critical velocity relative to the rotor.

$$T' - T'' = \left(T + \frac{\gamma-1}{\gamma} \frac{V^2}{2gR}\right) - \left(T + \frac{\gamma-1}{\gamma} \frac{W^2}{2gR}\right)$$

From figure 1 it can be seen that

$$V^2 = V_x{}^2 + V_u{}^2$$

and

$$W^2 = (V_u - u)^2 + V_x{}^2$$

where the direction of u is considered positive when viewed from a point on the stator.

Then

$$\frac{T''}{T'} = 1 + \frac{\gamma-1}{\gamma+1}\left[\left(\frac{u}{V_{cr}}\right)^2 - \frac{2V_u u}{V_{cr}^2}\right]$$

$$\frac{W_{cr}}{V_{cr}} = \sqrt{\frac{T''}{T'}} = \sqrt{1 + \frac{\gamma-1}{\gamma+1}\left[\left(\frac{u}{V_{cr}}\right)^2 - \frac{2V_u u}{V_{cr}^2}\right]} \qquad (7)$$

where

$$V_{u,4} = V_4 \sin \alpha$$

and

$$V_{u,5} = V_5 \sin \delta$$

The values of angles, velocities, and blade speeds were selected at the arithmetic mean radii to represent an average. The mean radii were 10.3 and 10.5 inches at stations 4 and 5, respectively.

Relative rotor flow angles. - The relative rotor-inlet and outlet flow angles can be found by means of the following relations (fig. 1):

$$\tan \beta = \tan \alpha - \left|\frac{u_4}{V_{x,4}}\right|$$

where

$$V_{x,4} = V_4 \cos \alpha$$

and

$$\tan \theta = \tan \delta + \left|\frac{u}{V_{x,5}}\right|$$

where

$$V_{x,5} = V_5 \cos \delta$$

RESULTS AND DISCUSSION

Power and Efficiency

The turbine-power parameter $(T'_3 - T'_5)/T'_3$ as a function of the total-pressure ratio across the turbine p'_3/p'_5 is plotted in figure 5. Lines of constant adiabatic efficiency were computed with a variation of the ratio of specific heats γ to correspond to the average encountered in the turbine investigations at each condition. The turbine efficiency ranged from 0.73 at the low pressure ratios to a maximum of approximately 0.85 at the design pressure ratio and decreased to 0.80 at high pressure ratios.

Weight Rate of Gas Flow through Turbine

The variation of the weight rate of gas flow through the turbine with the ratio of total inlet pressure to static back pressure is shown in figure 6. The corrected weight flow $w\sqrt{T'_3}/p'_3$ was multiplied by the corrected blade speed $u_{m,5}/\sqrt{T'_3}$ to correlate the data on one line. The data for all three jet-nozzle sizes fell within experimental accuracy of this line. The experimental value of the parameter $\dfrac{w\sqrt{T'_3}}{p'_3}\dfrac{u_{m,5}}{\sqrt{T'_3}}$ was, however, approximately 10 percent greater than the design value at corresponding ratios of total to static pressure. Aside from inaccuracies of weight-flow measurement, this discrepancy may be due to a larger effective flow area (less boundary layer) in the blade channels than was assumed in the design and also to some expansion of the blade-channel configuration due to high temperatures.

Weight-Flow Distribution at Stator-Cascade Outlet

Curves of weight flow per unit area (as measured in cascade tests at the stator outlet) as a function of stator-channel area measured perpendicular to the axis of rotation of the turbine are shown in figure 7. The inner radius of the air passages between blades was used as the origin of the graph, where channel area is zero, and the area increased in the outward radial direction until the total area of the channel was reached at the outer shroud or blade tip. Integration of the curve corresponding to the design

critical-velocity ratio of 0.80 yields a value of weight flow equal
to 94.8 percent of the value that would be obtained if the channel
were flowing full with no boundary layers. There is no appreciable
boundary layer at the outer shroud; however, a displacement thick-
ness of 0.16 inch was calculated at the inner shroud at the design
critical-velocity ratio. These values indicate that the design
assumption of boundary layers of 0.12 inch at the outer shroud and
0.30 inch at the inner shroud was quite pessimistic.

Stator and Rotor Flow Angles at Mean Radii

The stator-outlet angle α at the mean radius, as determined
from cascade data, was found to decrease from 66.0° to 62.5° between
the limits of critical-velocity ratio at the stator-cascade outlet
ranging from 0.41 to 0.96 (fig. 8). The air was underturned 2.3°
relative to the design value of 65.6°. The accuracy of measurement
in the cascade instrumentation was estimated to be $\pm 0.5^{\circ}$.

The variations of rotor-inlet and -outlet angles relative to
the rotor blades as computed from engine data in conjunction with
cascade data are presented in figure 9. The relative rotor-inlet
angle β varied almost linearly with the critical-velocity ratio
at the rotor outlet relative to the blades, the inlet angle decreas-
ing with increasing outlet critical-velocity ratio. The relative
rotor-outlet angle θ, computed by use of data taken at station 5,
shows hardly any variation with relative outlet critical-velocity
ratio within the experimental accuracy of the measurements, which
was estimated to be within $\pm 2^{\circ}$. The experimental results agreed with
the design value of relative rotor-outlet angle (63.3°) at the design
relative critical-velocity ratio (0.85) within experimental accuracy.
Thus both the stator and relative rotor-outlet angles were within
2.5° of the design values at the mean radii.

Neither the rotor-inlet nor -outlet angle was noticeably
affected by variation in jet-nozzle size. More significant, how-
ever, is the fact that the relative outlet angle remained constant
within 3° regardless of the rapidly decreasing relative inlet angle
with critical-velocity ratio. Further inspection of the data reveals
that, as the turbine-inlet temperature is increased (and thus blade
speed and weight flow are increased), the blade-speed component
(fig. 1) increases faster than the axial-speed component so that the
relative rotor-inlet angle is considerably reduced, whereas the
stator-outlet angle (fig. 8) is constant within approximately 4°.

Radial Distribution of Flow Angle at Stator-Cascade Outlet

Variation of the stator-outlet angle with radial position for four values of average stator-outlet critical-velocity ratio (0.41, 0.59, 0.80, and 0.96) is shown in figure 10. The dashed line indicates the design variation of outlet angle for an average outlet critical-velocity ratio of 0.8. The dashed line is drawn only within the limits of the assumed boundary layers. The air was slightly underturned over the major portion of the radial distance in comparison with the design curve; the degree of underturning increased with radial distance. The stator-outlet angle decreased too rapidly with radial distance from the hub to correspond to a free-vortex flow distribution. The outlet angle, however, was sharply increased in the inner boundary layer.

Radial Distribution of Rotor-Outlet Flow Angle

The radial distribution of absolute rotor-outlet angle δ is presented in figure 11 for a jet nozzle 15.97 inches in diameter. For this nozzle size, the turbine operated over a range of blade speed divided by relative critical velocity $\dfrac{u_5}{W_{cr,m,5}}$ of 0.37 to 0.55 and over a corresponding range of relative rotor-outlet critical-velocity ratios $\dfrac{W_{m,5}}{W_{cr,m,5}}$ of 0.58 to 0.95. The design curve $\dfrac{u_5}{W_{cr,m,5}} = 0.54$ is shown on the figure by a dashed line. Interpolated experimental results near a value of $\dfrac{W_{m,5}}{W_{cr,m,5}} = 0.85$ followed the design curve within 3° for the first three-fourths of the radial distance from the hub or inner shroud. Near the blade tip or outer shroud, however, the outlet angle decreased considerably, which probably was caused by the large blade-tip clearance of 0.10 inch.

Radial Distribution of Total Pressures at Stator-Cascade Outlet

The stator was designed for a uniform distribution of total pressure between an inner boundary layer of 0.30 inch and an outer boundary layer of 0.12 inch. Figure 12 shows that this condition was obtained in the cascade tests of the stator blades with only

5-percent variation occurring near the limits of the design radial distance, as shown by the dashed line. Total pressure dropped rapidly near the inner shroud, however.

Radial Distribution of Rotor-Outlet Pressure

The radial distribution of rotor-outlet total pressure (relative to a stationary part of the turbine) is given in figure 13 for a jet nozzle 15.97 inches in diameter. The total pressure was quite constant between the radii of 9.25 and 11.25 inches. The total pressure decreased quite rapidly at the inner radii. Not enough data were available to calculate the boundary-layer displacement thickness. The total pressure at the outer radii decreased because of the rotor-blade-tip clearance.

SUMMARY OF RESULTS

A preliminary investigation made of the first stage of a two-stage turbine designed for free-vortex flow, matched to a centrifugal compressor, and operated in conjunction with combustors, engine accessories, and three sizes of jet nozzle gave the following results:

1. The variables studied in this investigation approximated the turbine design conditions as follows:

(a) Adiabatic efficiency was about 0.05 lower than the design value of 0.90, peak efficiency occurring when the turbine was operating near the design total-pressure ratio.

(b) The experimental value of the weight-flow parameter was approximately 10 percent greater than the design value at corresponding values of the ratio of total inlet to static back pressure.

(c) Boundary-layer displacement thickness at the stator outlet was 0.16 inch at the hub and negligible at the tip compared with a design value of 0.30 inch at the hub and 0.12 inch at the tip.

(d) The stator- and rotor-outlet flow angles at the mean radii were within 2.5° of the design values.

2. The turbine blading performed as.follows over the range of variables investigated:

(a) Relative rotor-outlet angles remained constant within 2.5°, although the relative rotor-inlet angle varied 16°.

(b) The stator-outlet angle decreased too rapidly with radial distance from the hub to correspond to a free-vortex flow distribution.

(c) The radial distribution of absolute rotor-outlet angle followed the design curve within 3° for the first three-fourths of the radial distance from the hub after which the angle decreased rapidly because of an excessive rotor-blade-tip clearance.

(d) Radial distributions of total pressure at the stator and rotor outlets were uniform within experimental accuracy over the major portion of the radial distances.

Lewis Flight Propulsion Laboratory,
    National Advisory Committee for Aeronautics,
        Cleveland, Ohio, November 21, 1949.

REFERENCES

1. Liepmann, Hans Wolfgang, and Puckett, Allen E.:   Introduction to
    Aerodynamics of a Compressible Fluid. John Wiley & Sons, Inc.,
    1947, pp. 23-24.

2. Goldstein, Arthur W.: Analysis of Performance of Jet Engine from
    Characteristics of Components. I - Aerodynamic and Matching
    Characteristics of Turbine Component Determined with Cold Air.
    NACA Rep. 878, 1947. (Formerly NACA TN 1459.)

3. Huppert, M. C., and MacGregor, Charles: Comparison between Pre-
    dicted and Observed Performance of Gas-Turbine Stator Blade
    Designed for Free-Vortex Flow. NACA TN 1810, 1949.

TABLE I - DIMENSIONS TO DETERMINE BLADE PROFILES

[All dimensions in inches]

(a) Stator-blade profile coordinates.

X	Root-section radius, 9.3		Mean-section radius, 10.3		Tip-section radius, 11.5	
	Y_1	Y_2	Y_1	Y_2	Y_1	Y_2
0	0.060	-0.053	0.060	-0.053	0.060	-0.053
.100	.115	-.069	.115	-.069	.115	-.069
.200	.150	-.088	.149	-.085	.148	-.083
.300	.170	-.110	.167	-.105	.165	-.100
.400	.178	-.138	.173	-.130	.168	-.123
.500	.172	-.172	.165	-.162	.158	-.152
.600	.152	-.212	.143	-.199	.135	-.187
.700	.119	-.258	.108	-.244	.097	-.230
.800	.065	-.317	.053	-.299	.042	-.282
.900	-.012	-.387	-.020	-.365	-.029	-.344
1.000	-.115	-.471	-.115	-.443	-.114	-.415
1.100	-.247	-.570	-.230	-.533	-.213	-.497
1.200	-.412	-.690	-.373	-.641	-.335	-.592
1.300	-.615	-.836	-.544	-.771	-.473	-.706
1.400	-.871	-1.025	-.756	-.935	-.641	-.845
1.500	-1.175	-1.247	-1.000	-1.119	-.845	-1.005
1.600					-1.105	-1.182
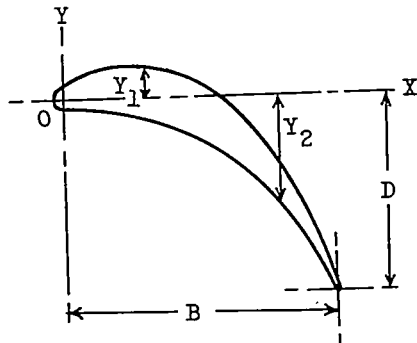
Leading-edge radius, 0.050
Trailing-edge radius, 0.0075
Origins of three two-dimensional
    sections are alined on common
    radial line passing through
    axis of rotation of turbine
B axial distance between centers
    of leading and trailing edges
D normal distance between centers
    of leading and trailing edges

(b) Characteristic dimensions of stator.

	Root-section radius, 9.3	Mean-section radius, 10.3	Tip-section radius, 11.5
Chord length	2.038	2.070	2.094
Solidity	1.709	1.563	1.420
Axial distance, B	1.524	1.575	1.630
Normal distance, D	1.266	1.254	1.222

TABLE I - DIMENSIONS TO DETERMINE BLADE PROFILES - Concluded

[All dimensions in inches]

(c) Rotor-blade profile coordinates.

X	Root-section radius, 9.3		Mean-section radius, 10.5		Tip-section radius, 11.5	
	Y_1	Y_2	Y_1	Y_2	Y_1	Y_2
0	0.509	0.120	0.517	0.172	0.524	0.223
.100	.523	.130	.532	.188	.540	.247
.200	.522	.132	.533	.198	.544	.263
.300	.507	.126	.521	.198	.535	.270
.400	.477	.112	.495	.192	.513	.272
.500	.430	.090	.453	.180	.476	.269
.600	.364	.059	.393	.158	.422	.257
.700	.279	.020	.310	.125		
.800	.170	-.023				
-.100	.481	.101	.485	.142	.489	.184
-.200	.438	.070	.436	.100	.434	.130
-.300	.380	.029	.370	.047	.359	.064
-.400	.303	-.027	.282	-.021	.260	-.015
-.500	.203	-.097	.165	-.106	.126	-.116
-.600	.075	-.184	.023	-.212	-.029	-.239
-.700	-.088	-.292	-.154	-.338	-.220	-.384
-.800	-.285	-.416	-.368	-.485	-.452	-.554
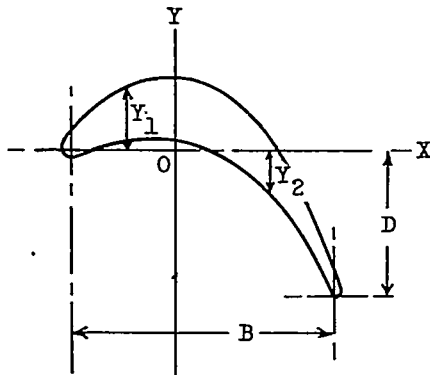
Leading-edge radius, 0.050
Trailing-edge radius, 0.012
Origins of three two-dimensional
   sections are alined on common
   radial line passing through axis
   of rotation of turbine
B axial distance between centers
   of leading and trailing edges
D normal distance between centers
   of leading and trailing edges

(d) Characteristic dimensions of rotor.

	Root-section radius, 9.3	Mean-section radius, 10.5	Tip-section radius, 11.5
Chord length	1.866	1.856	1.868
Solidity	1.724	1.524	1.396
Axial distance, B	1.734	1.640	1.546
Normal distance, D	.499	.726	.933
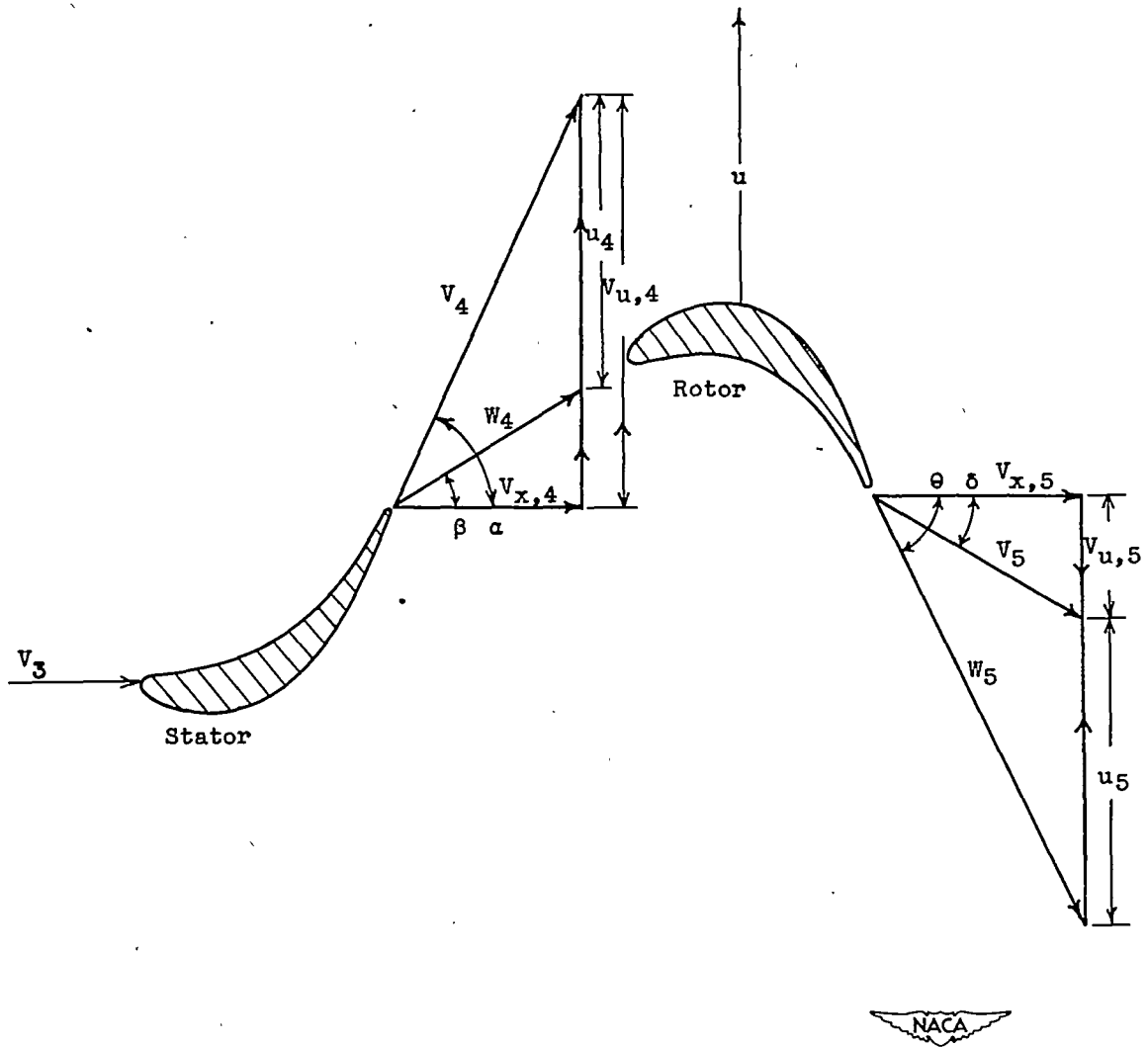
Figure 1. - General velocity distribution in single-stage turbine.
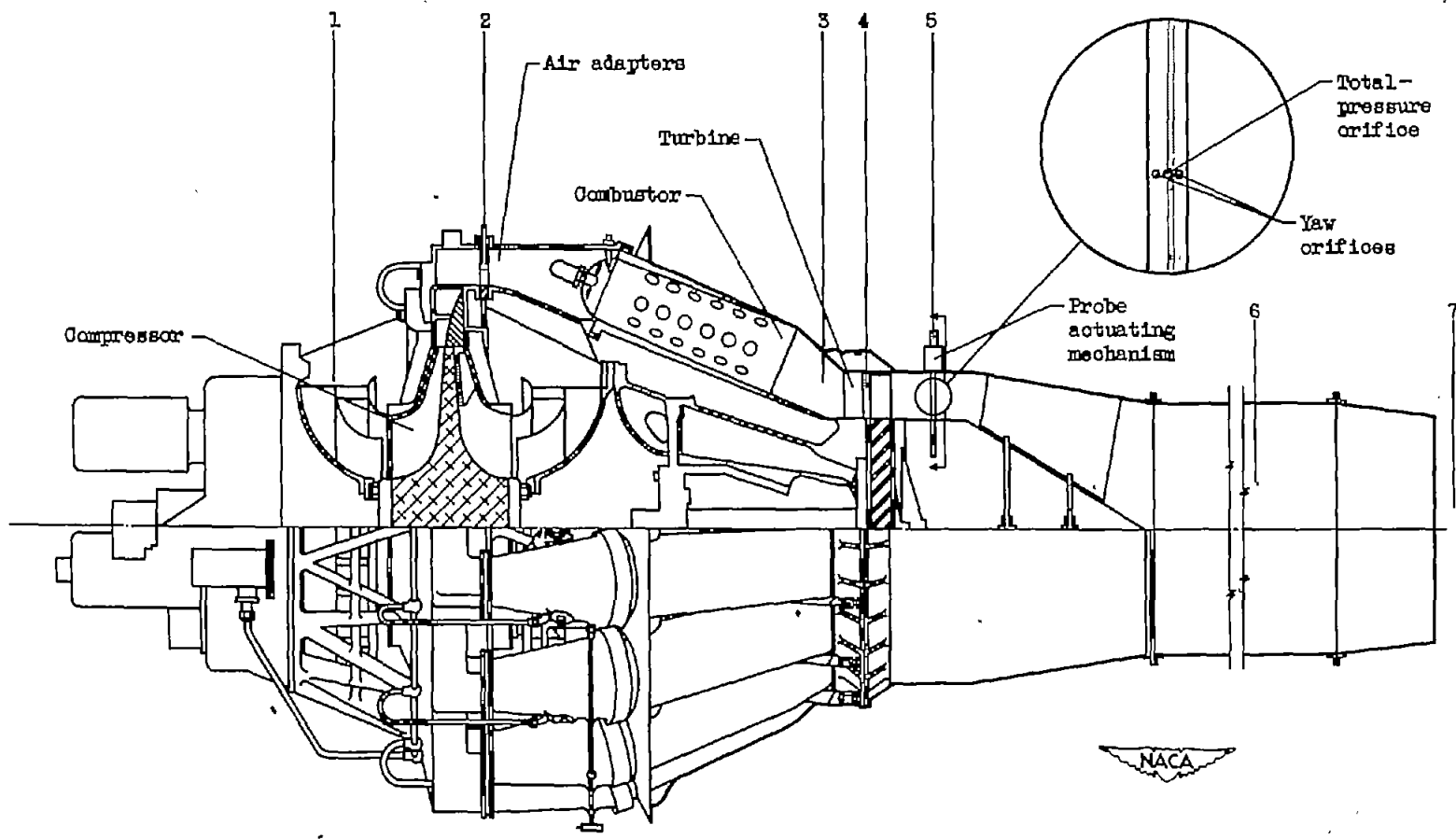
Figure 2. - General configuration of turbojet engine showing position of measuring stations.
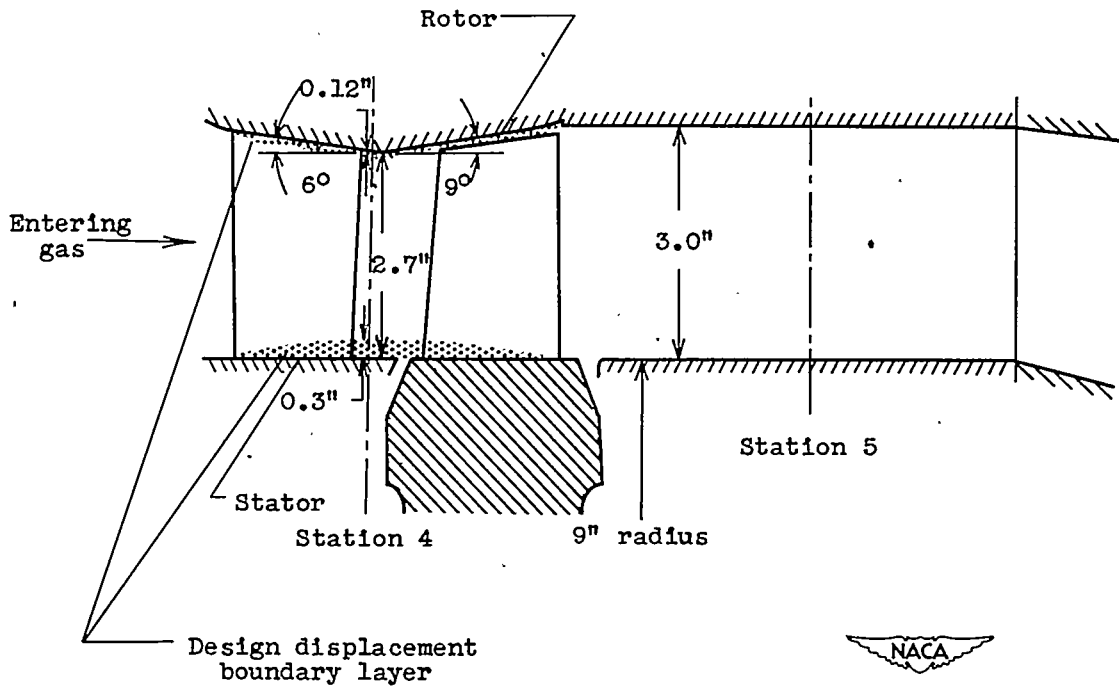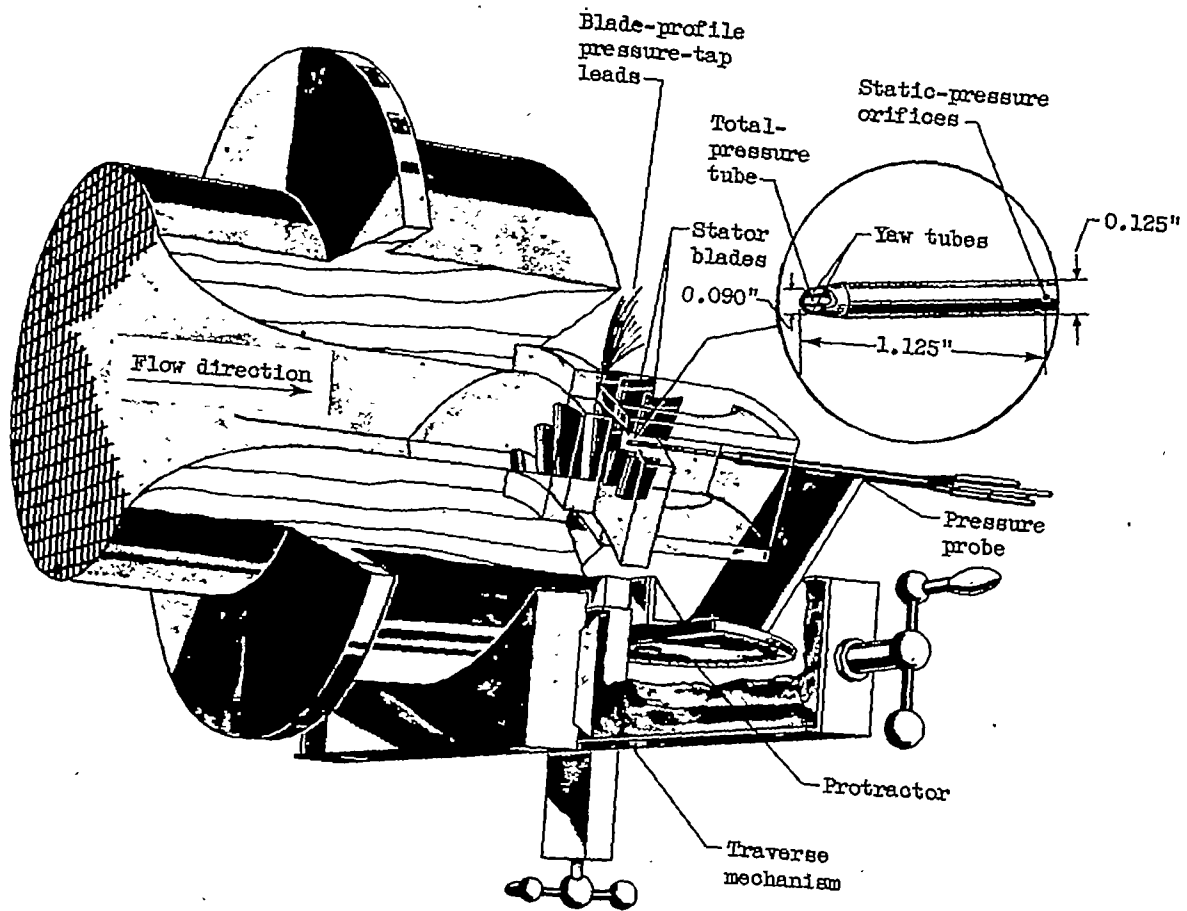
Figure 3. - Side view of turbine flow passage.

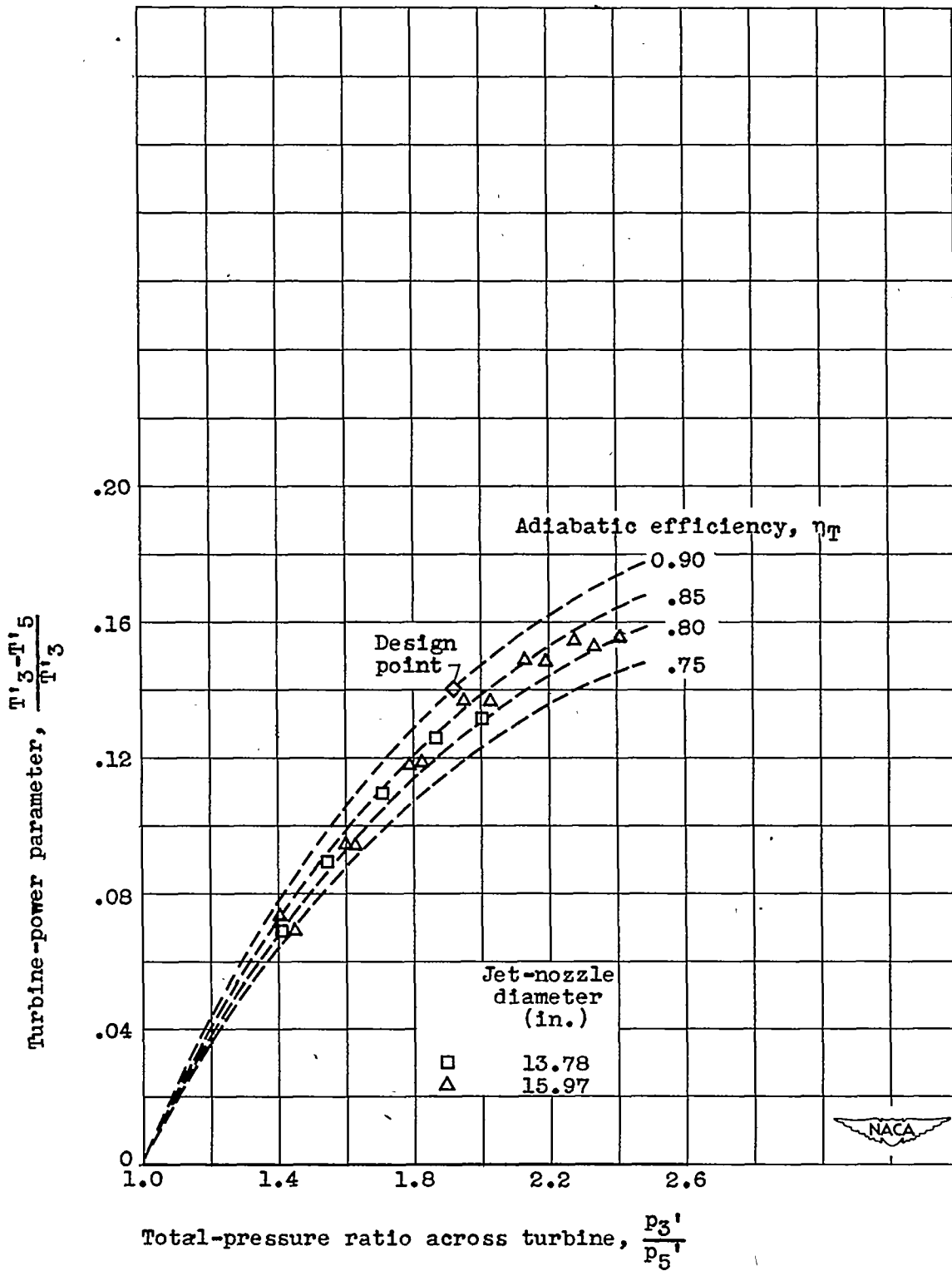Figure 4. - Stator-flow test assembly.

Figure 5. - Variation of turbine-power parameter
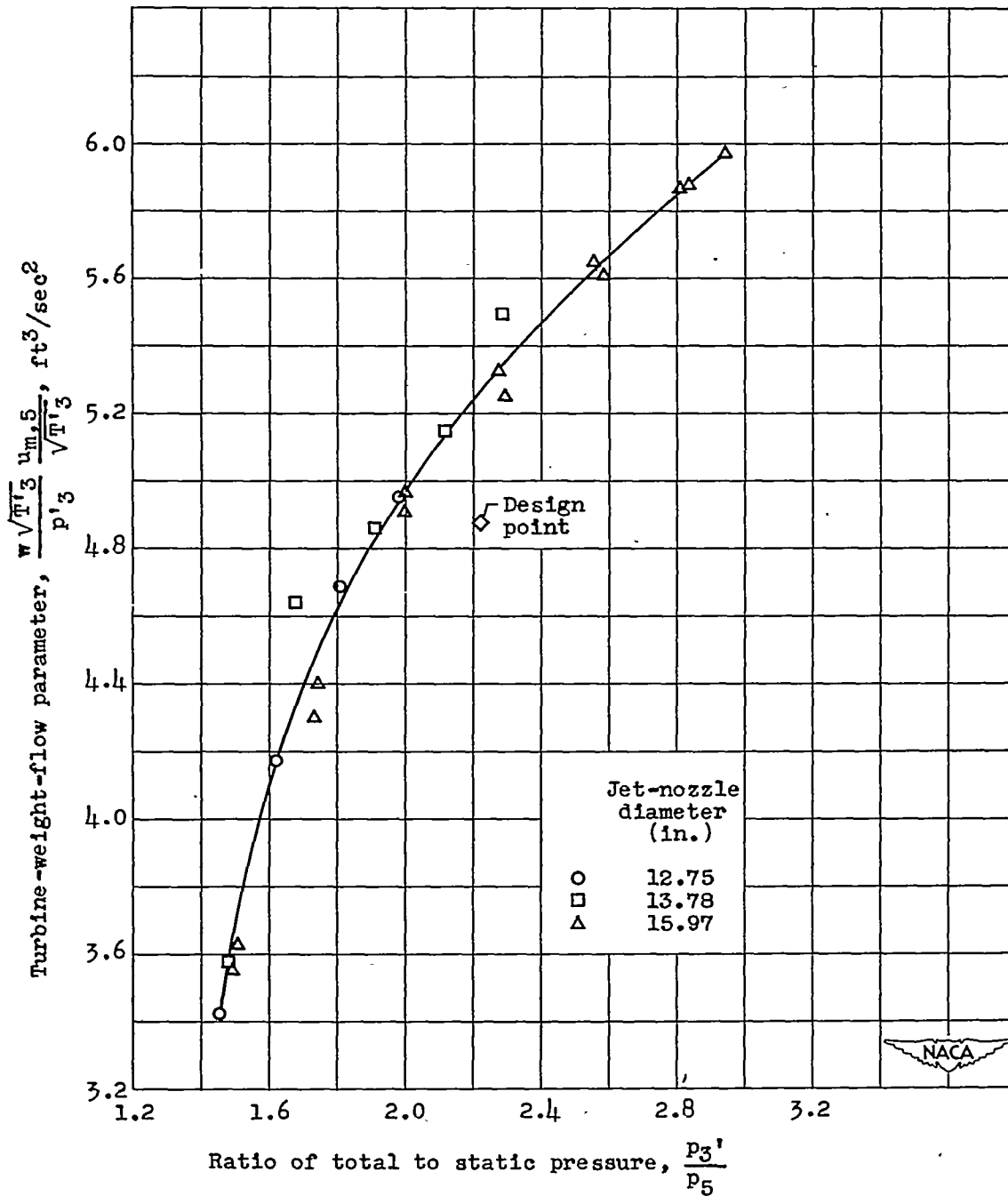with total-pressure ratio across turbine.

Figure 6. – Variation of weight-flow parameter with ratio
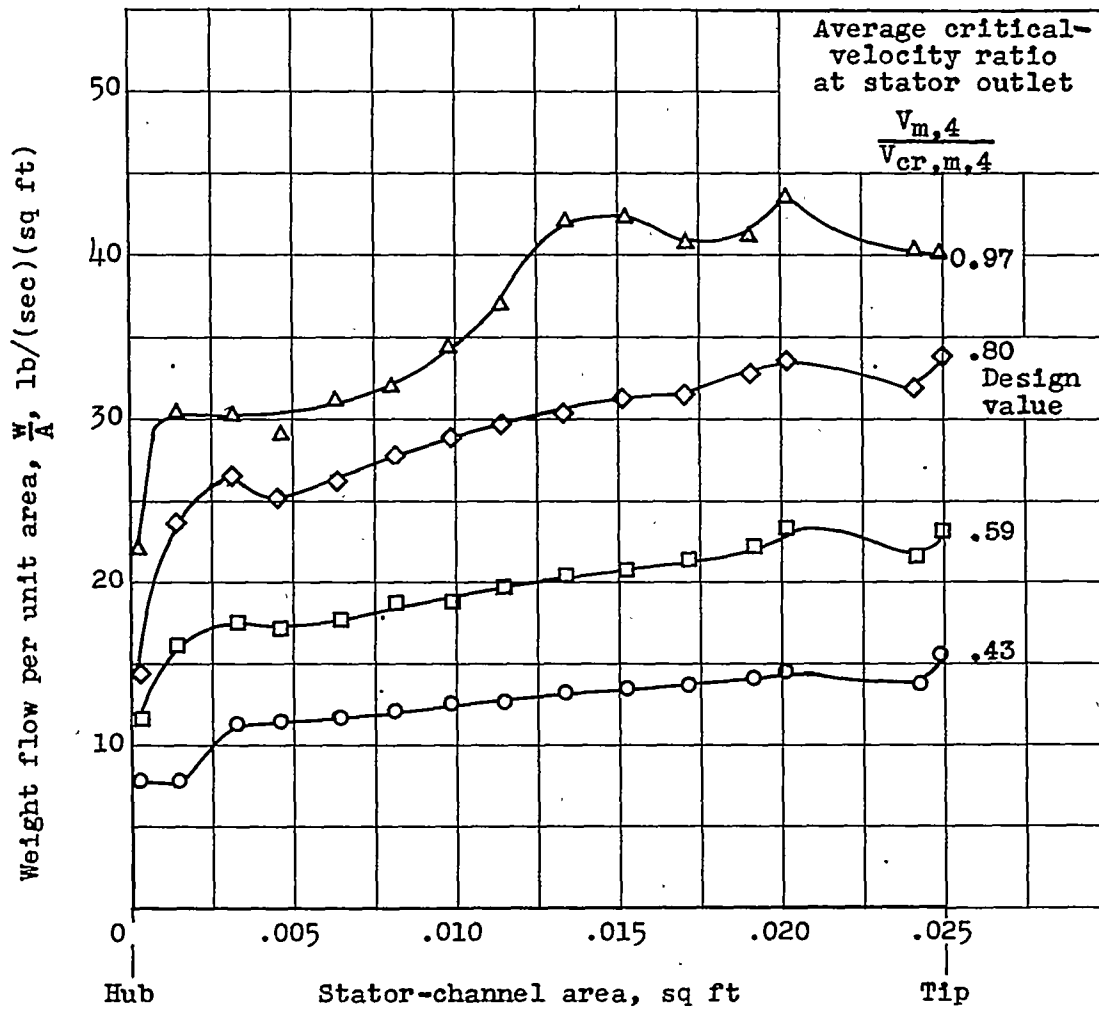of total to static pressure across turbine.

Figure 7. - Variation of weight flow per unit channel area for various values of average critical-velocity ratio at stator-cascade outlet.
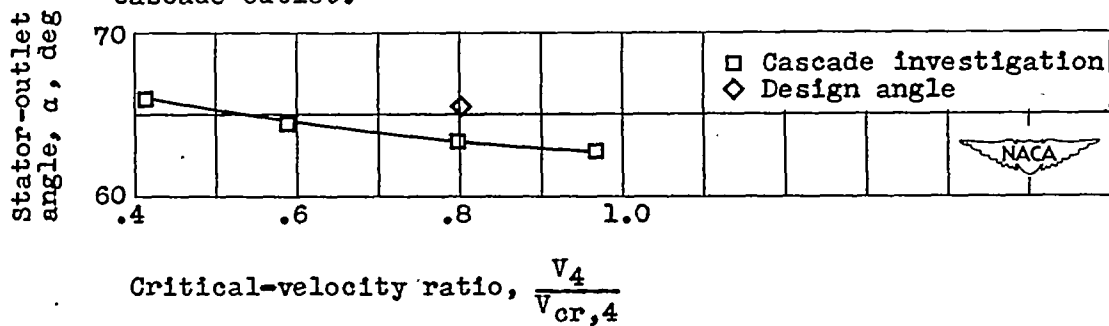
Figure 8. - Variation of stator-outlet angle with critical-velocity ratio at mean radius of stator-cascade outlet.
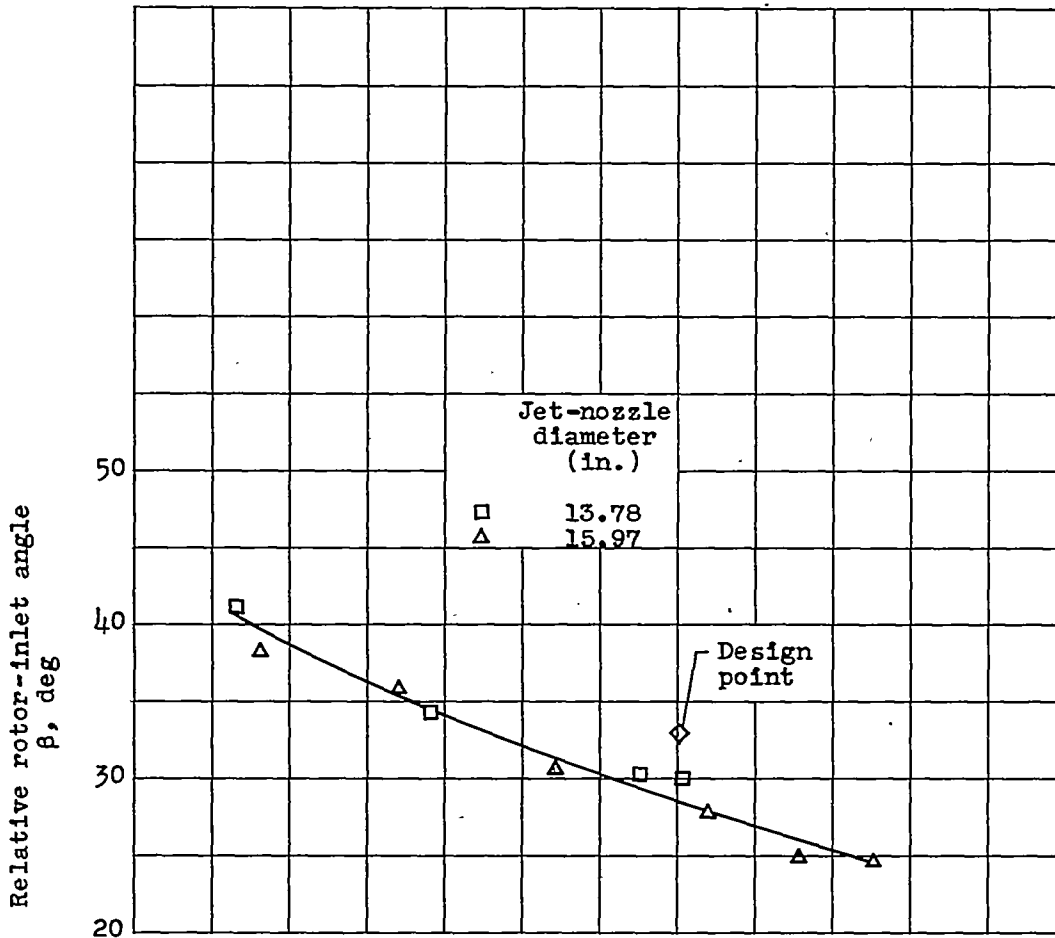
(a) Rotor-inlet angle.
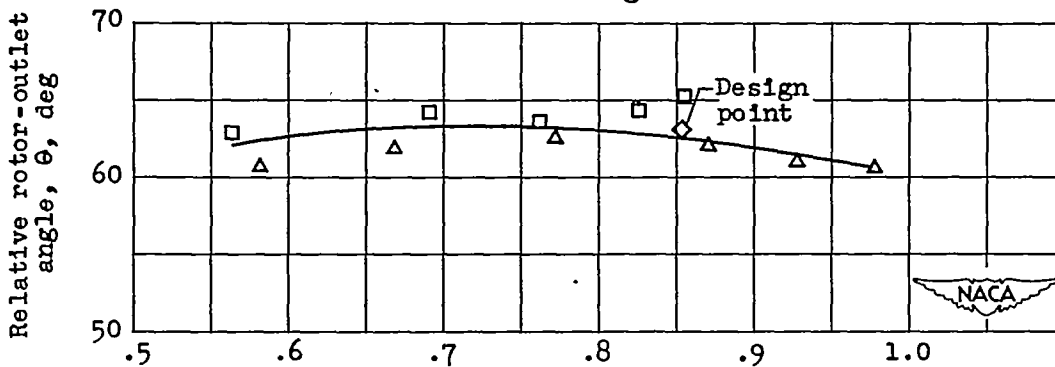
(b) Rotor-outlet angle.

Figure 9. - Variation of rotor-inlet and -outlet angles
relative to rotor at mean radius of rotor as function
of relative critical-velocity ratio.
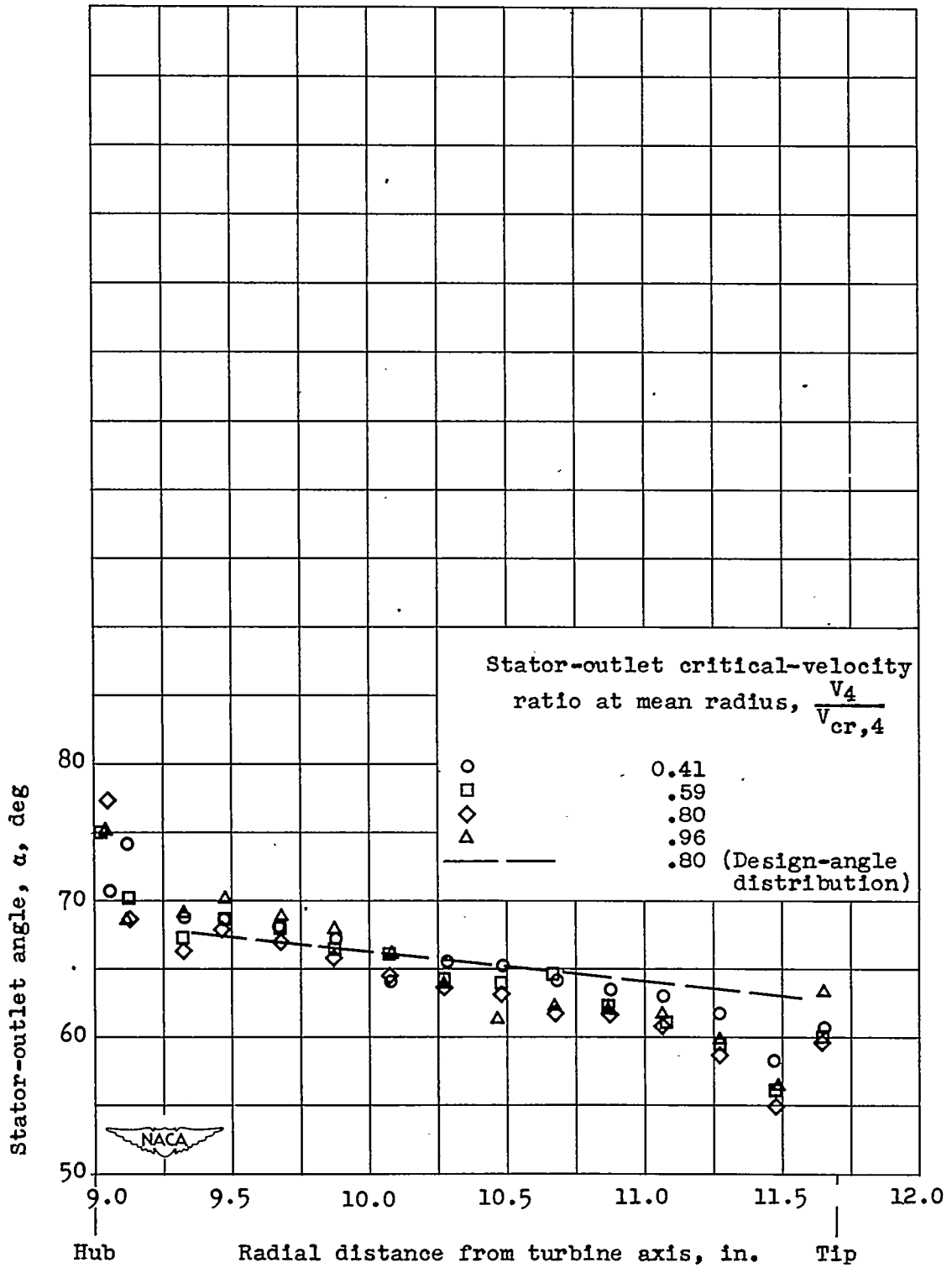
Figure 10. - Radial distribution of flow angle at stator-cascade outlet.
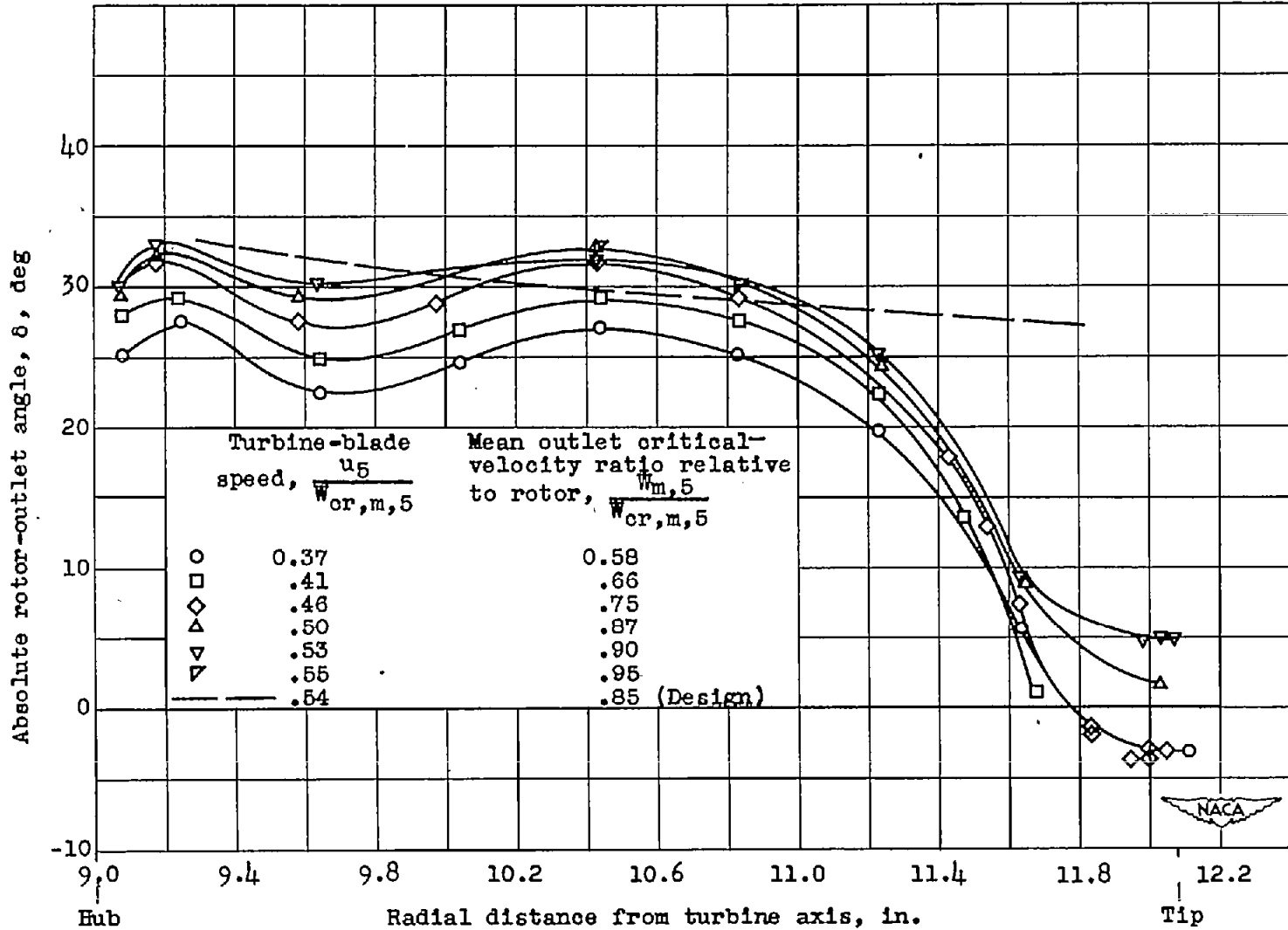
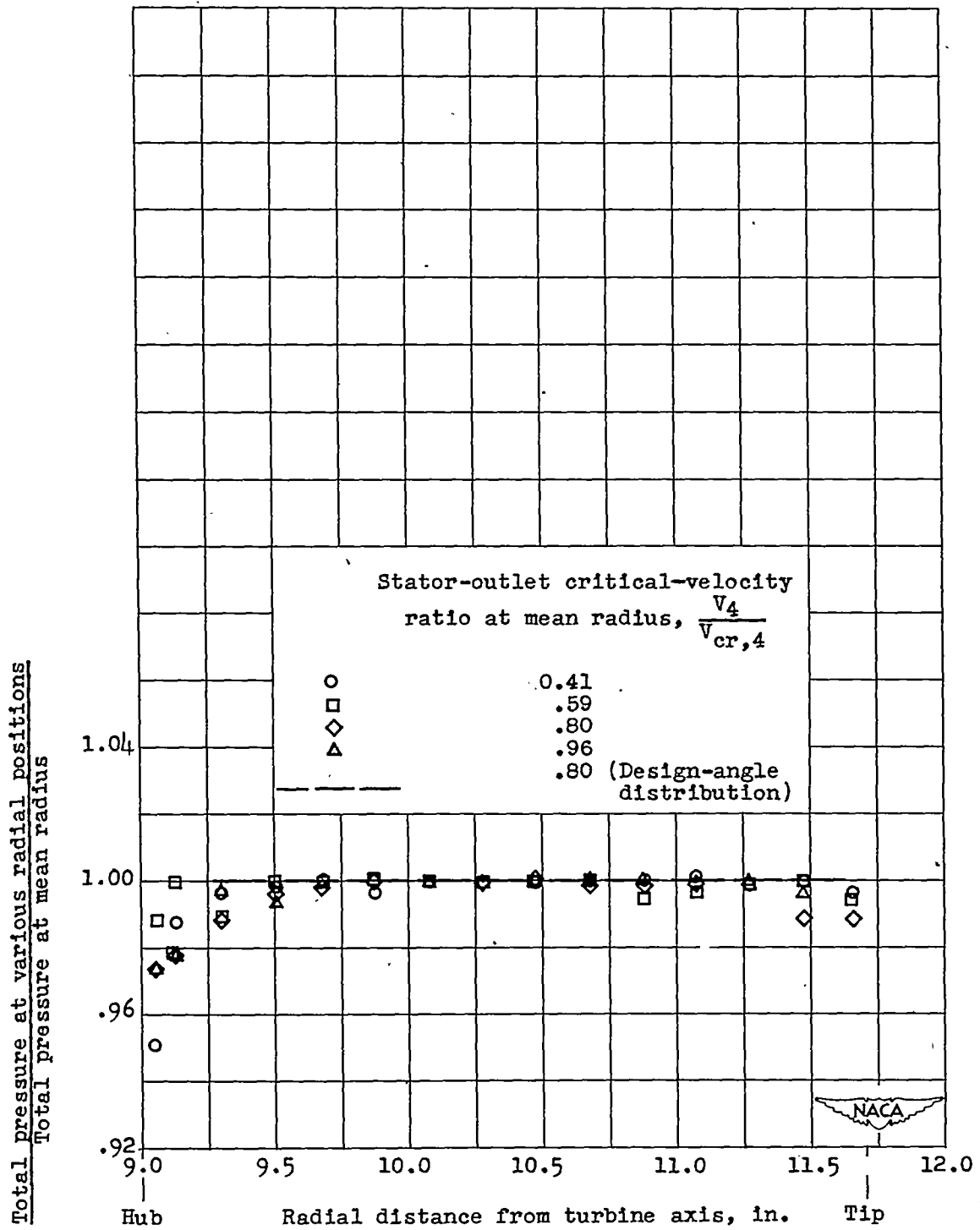Figure 11. - Radial distribution of absolute rotor-outlet flow angle.   Jet-nozzle diameter, 15.97 inches.

Figure 12. - Radial distribution of total pressure at outlet of
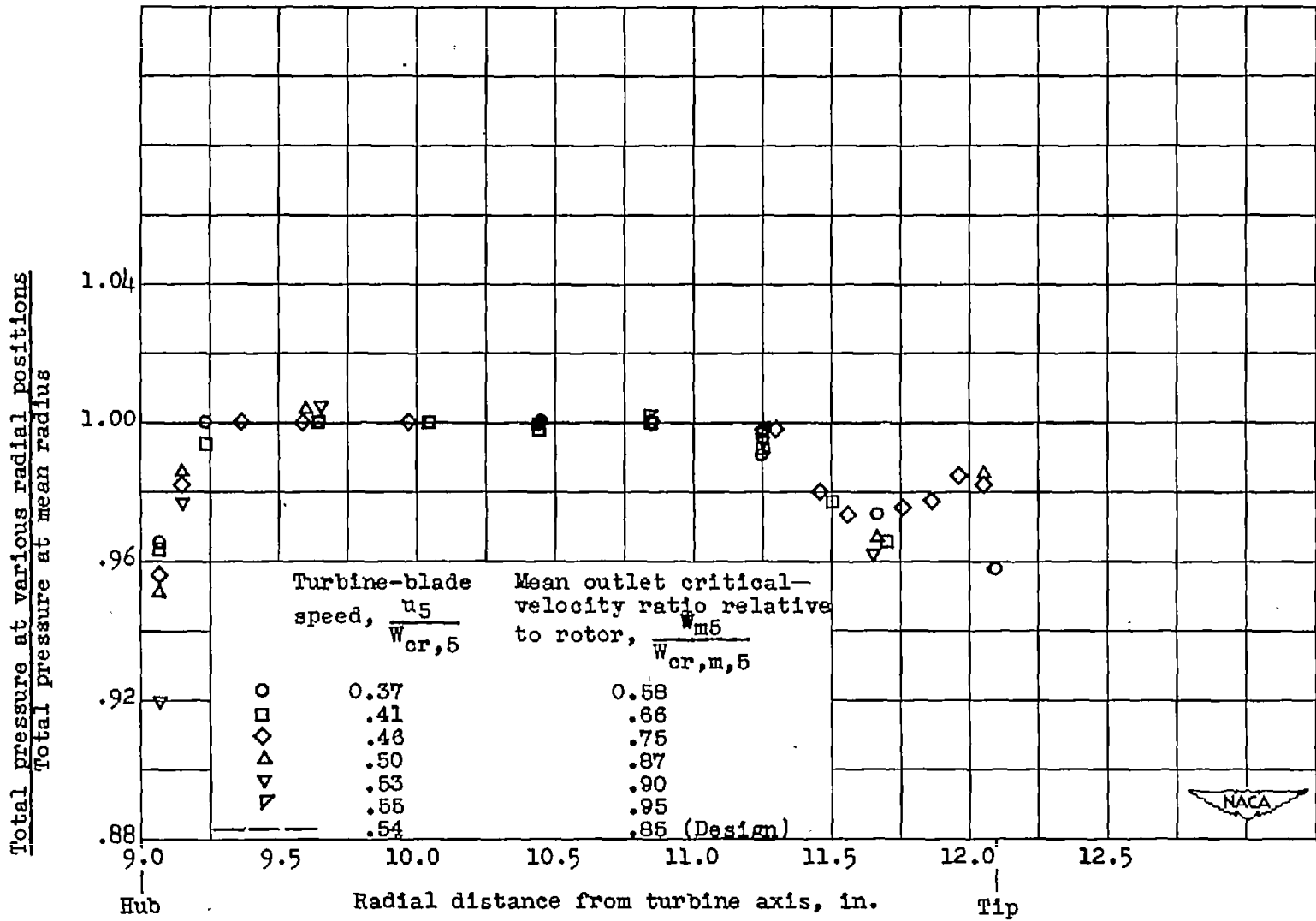stator cascade.

Figure 13. - Radial distribution of total pressure at outlet of rotor. Jet-nozzle diameter, 15.97 inches.